

# **Effect of homogenization on anodic film and electrochemical behavior of an A535 alloy after sealing with stearic sealant**

Suwaree Chankitmunkong, Dmitry G. Eskin, Chaowalit Limmaneevichitr, Phromphong Pandee, Nattarat Kengkla, Jirakit Athchasisri, Tanawat Tanawansombat, Napadol Parnlasarn, Onnjira Diewwanit

Suwaree Chankitmunkong

Department of Industrial Engineering, School of Engineering, King Mongkut's Institute of Technology Ladkrabang, Chalongkrung Road, Ladkrabang, Bangkok 10520 Thailand

e-mail: suwaree.ch@kmitl.ac.th

Dmitry G. Eskin

Brunel University London, BCAST, Uxbridge, Middlesex UB8 3PH, United Kingdom

Tomsk State University, Tomsk 634050, Russian Federation

e-mail: dmitry.eskin@brunel.ac.uk

Chaowalit Limmaneevichitr

Department of Production Engineering, Faculty of Engineering, King Mongkut's University of Technology Thonburi, Pracha-Utid Road, Bangmod, Tungkhru, Bangkok 10140, Thailand

e-mail: chaowalit.lim@mail.kmutt.ac.th

Phromphong Pandee

Department of Production Engineering, Faculty of Engineering, King Mongkut's University of Technology Thonburi, Pracha-Utid Road, Bangmod, Tungkhru, Bangkok 10140, Thailand

e-mail: phrompong.pan@mail.kmutt.ac.th

Nattarat Kengkla

Department of Tool and Materials Engineering, Faculty of Engineering, King Mongkut's University of Technology Thonburi, Pracha-Utid Road, Bangmod, Tungkhru, Bangkok 10140, Thailand

e-mail: nattaratkengkla@hotmail.com

Jirakit Athchasisri

Department of Tool and Materials Engineering, Faculty of Engineering, King Mongkut's University of Technology Thonburi, Pracha-Utid Road, Bangmod, Tungkhru, Bangkok 10140, Thailand

e-mail: Ken\_jirakit@hotmail.com

Tanawat Tanawansombat

Department of Tool and Materials Engineering, Faculty of Engineering, King Mongkut's University of Technology Thonburi, Pracha-Utid Road, Bangmod, Tungkhru, Bangkok 10140, Thailand

e-mail: Mart\_2012@hotmail.co.th

Napadol Parnlasarn

Department of Tool and Materials Engineering, Faculty of Engineering, King Mongkut's University of Technology Thonburi, Pracha-Utid Road, Bangmod, Tungkhru, Bangkok 10140, Thailand

e-mail: napadol.parnlasarn@gmail.com

Onnjira Diewwanit

Department of Tool and Materials Engineering, Faculty of Engineering, King Mongkut's University of Technology Thonburi, Pracha-Utid Road, Bangmod, Tungkhru, Bangkok 10140, Thailand

e-mail: onnjira.tha@kmutt.ac.th

## **Abstract**

Almag 35 (A535) is a commercial aluminum alloy intended for a number of marine components, which is mainly justified by its excellent castability and corrosion resistance. However, the most important factor for corrosion resistance is the formation of intermetallics that can lead the defects in the oxide film and substrate, as well as activate the corrosion reaction. The characteristics of a sealant on the anodic film was investigated in this work. The alloy was subjected to homogenization at 400 °C for 5 hours to improve the uniformity of the anodic oxide film due to the decreased number of intermetallics as a result of dissolving in the matrix. It also improved the hardness of this alloy. Electrochemical measurements were conducted to investigate the corrosion behavior. The effects of intermetallics and stearic sealing on characteristics of the oxide layer are discussed. The decrease in a number of intermetallics can lead to the reduced

corrosion current density ( $I_{\text{corr}}$ ) and increased potential corrosion ( $E_{\text{corr}}$ ), which results in a lower corrosion rate of this alloy.

Keywords: Al-Mg alloy, Anodic film, Anodic sealing, Corrosion, Stearic acid, Homogenization

## Introduction

An A535 aluminum–magnesium casting alloy is widely used in marine applications due to good castability, high strength-to-weight ratio and excellent corrosion resistance [1]. However, unlike wrought aluminum alloys, this alloy is normally used to produce as-cast final products without homogenization treatment [2]. Thus, such an alloy with high Mg content may become highly susceptible to intergranular corrosion as a result of the formation of intermetallic  $\text{Al}_3\text{Mg}_2$  precipitates at grain boundaries [3]. In practice, aluminum casting alloys are used as near-net shape products with a surface coating by painting for improving the corrosion resistance [4]. However, this technique has a lower performance than anodizing coating as the latter can provide a strong oxide film that can be further improved by sealing treatment, i.e. by chemical reaction of an organic sealant such as stearic acid that can reduce the porosity of the oxide layer [5]. Despite anodizing being one of the common surface treatments employed to improve corrosion resistance of Al alloys [6], some alloys such as Al-Cu, Al-Zn and Al-Mg alloys are not compatible as they exhibit intermetallics and have high levels of ion entrainment in the anodizing film, which results in the uneven and limited growth and poor quality of the oxide film [7]. Homogenizing heat treatment of as-cast Al alloys mainly targets the dissolution of excess phases and decreasing elemental microsegregation, grain boundary segregation and changing the shape of intermetallics that are formed during solidification; ensuring a more uniform solid solution before further processing or surface treatment [8, 9]. Therefore, the objective of this work is to investigate the effects of homogenization in an A535 aluminum–magnesium casting alloy on the microstructure, hardness and capability of anodizing process with stearic sealing, which can positively affect corrosion resistance and behavior.

## Experiments

An A535 aluminum–magnesium casting alloy was prepared in an induction furnace at a temperature of 750 °C and then poured into a permanent steel mold (width 100 mm, height 200 mm and 17 mm in thickness). The cast alloy was cut into small pieces of 25 mm x 25 mm x 17 mm in dimensions before homogenization at 400 °C for 5 to 7 hours following [10]. The typical nominal composition of the alloy as obtained from a spark optical emission spectrometer (ARL 3460 model) and the surface treatment conditions of the alloy are given in Table 1.

Selected samples were ground and polished to observe the microstructure and intermetallics by an optical microscope. The area fraction of intermetallics was measured by image analysis using Image J software. The hardness of the alloy was determined by a Rockwell (HRB)/Rockwell Superficial- Wolpert using a ball diameter of 1.5875 mm under a load of 980.7 N. Five measurement were conducted for the statistically valid value.

The as-cast and homogenized alloys were etched in an alkaline solution by immersion in 5 wt% sodium hydroxide solution at 45-50 °C before desmutting by immersion in 25 vol.% nitric acid for 2 min and DI water for 30 sec. After that, the samples were anodized in a mixed electrolyte

of 175 g/l sulfuric acid, 0.16 mol/l aluminum sulfate and 30 g/l of oxalic acid and sealed with stearic sealant. The surface morphology of the anodic oxide film was investigated by using a scanning electron microscope (JEOL-JSM-6610 LV)

To study the corrosion behavior of the alloy, the potentiodynamic polarization corrosion test was performed by using a potentiostat-galvanostat model Autolab P302N in a three-electrode system. Tafel polarization curves were recorded, where the considerable information on the electrode process can be obtained as corrosion current density ( $I_{\text{corr}}$ ) and corrosion potential ( $E_{\text{corr}}$ ). The obtained current density from the Tafel polarization curves was used to calculate the corrosion rate following the ASTM G102-89 standard [11].

**Table 1** Chemical composition and surface coating with anodizing and sealing conditions

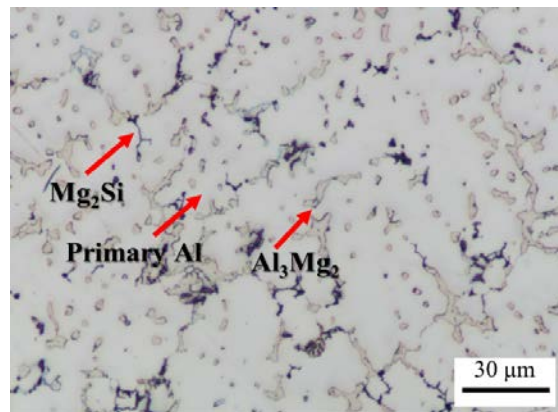
Alloy	Chemical Composition (wt%)							
	Al	Mg	Mn	Si	Fe	Ti	Ni	Cu
A535	Bal.	6.6	0.25	0.23	0.14	0.05	0.01	0.0001

Specimens	Conditions
CA	As-cast + Anodized
HA	As-cast + Homogenized + Anodized
CAS	As-cast + Anodized + Stearic Sealed
HAS	As-cast + Homogenized + Anodized + Stearic Sealed

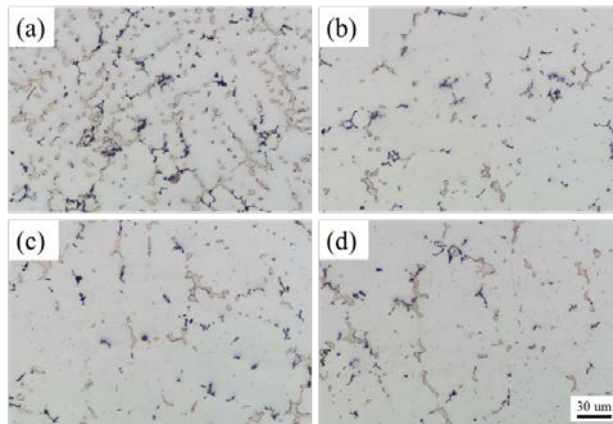
## Results and Discussion

Figure 1 shows that the initial microstructure of an as-cast A535 alloy consisted of  $\text{Mg}_2\text{Si}$  and  $\text{Al}_3\text{Mg}_2$  particles distributed in the Al matrix. It can be seen that these phases formed as divorced eutectics at the grain boundaries and in the interdendritic region.



**Fig.1** Microstructure of an as-cast A535 casting alloy.

The effects of homogenization time on the microstructure of an A535 alloy is demonstrated in Fig. 2. In general, the intermetallics appeared to be smaller and more evenly distributed in the Al matrix after homogenization for 5 hours. As the dissolution of  $Mg_2Si$  and  $Al_3Mg_2$  in the aluminum matrix progressed, the number of intermetallics significantly decreased. However, the longer homogenization duration (6-7 hours) did not significantly affect the dissolution of these intermetallics. The overall amount of intermetallics decreased from appr. 20 vol.% to 10 vol.% after 5-7 hours annealing, as can be seen in the changes of the area fractions in Fig. 3.



**Fig. 2** Microstructure of the alloy: (a) without homogenization, and homogenized at 400 °C for (b) 5 hours, (c) 6 hours. and (d) 7 hours.

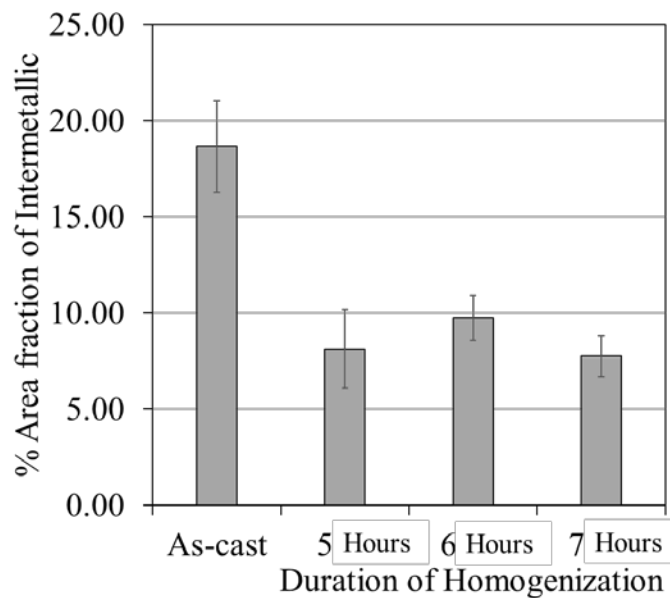


**Fig. 3** Percent area fraction of intermetallics in the as-cast and as-homogenized samples at different annealing times

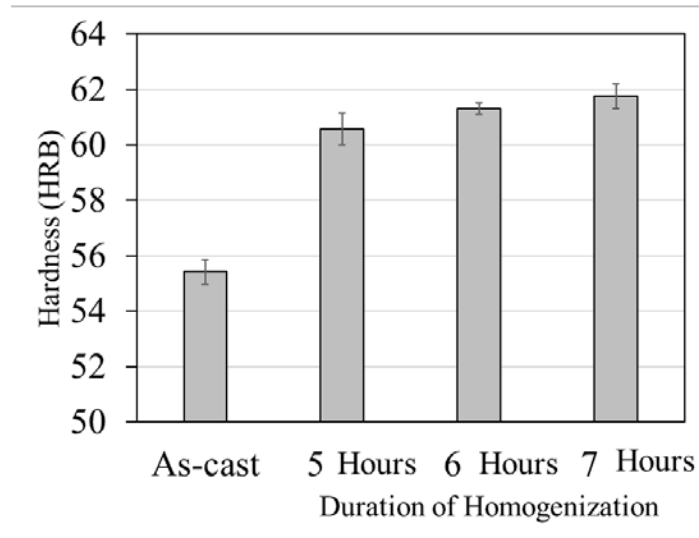


**Fig.4** Hardness of A535 specimens in as-cast and as-homogenized conditions

Figure 4 shows the hardness of the alloy after casting and homogenization at 400 °C for 5 to 7 hours. The hardness significantly increased from about 55 HRB to 62 HRB. This is a direct result of intermetallic phases dissolution in aluminum during homogenization, increasing the concentration of Mg and Si solute atoms in the aluminum matrix. These Mg and Si solute atoms promoted the solid solution strengthening [12]. The result also showed that the longer exposure time of homogenization treatment is not influencing greatly the increment of hardness. As a result of the structure and hardness examination, the homogenization at 400 °C for 5 hours was used further for preparing the specimens that were subjected to anodizing and sealing to investigate the corrosion behavior of this alloy.

The cross-section and the thickness of anodic oxide film in as-cast and homogenized specimens with and without stearic sealing are illustrated in Fig. 5. The result showed that the amount of intermetallics that are embedded in the cross-sectional anodic film was less when the alloy was homogenized at 400 °C for 5 hours before anodizing. The average thickness of the oxide film increased from 42 μm to about 50 μm in the homogenized alloy without stearic sealing as shown in Fig. 5 (a) and (b). It was reported that high concentration of secondary phases leads to defects in the oxide film layer [13]. Moreover, the thickness of the anodic oxide film depends on holding time during anodizing and the amount of secondary phases [13] and on the sealing [14]. The stearic sealing in the homogenized alloy increased the thickness of the oxide film up to 70 microns as compared to the sealing of the as-cast alloy, as can be clearly seen in Fig. 5 (c) and (d). This can be explained by the two possible reasons, i.e. (i) the stearic sealing is a thermal chemical reaction process that can stimulate the growth of the oxide film and form an aluminum soap petal-shaped layer on the surface [5, 14], and (ii) the lesser amount of intermetallics in the homogenized alloy may accelerate the growth of the oxide film [15]. The observation of the anodic oxide film thickness is in good agreement with the literature that reports that the initial dissolution of intermetallics plays a significant role in the growth of anodic film that exhibits more uniformity in homogenized alloys [15].

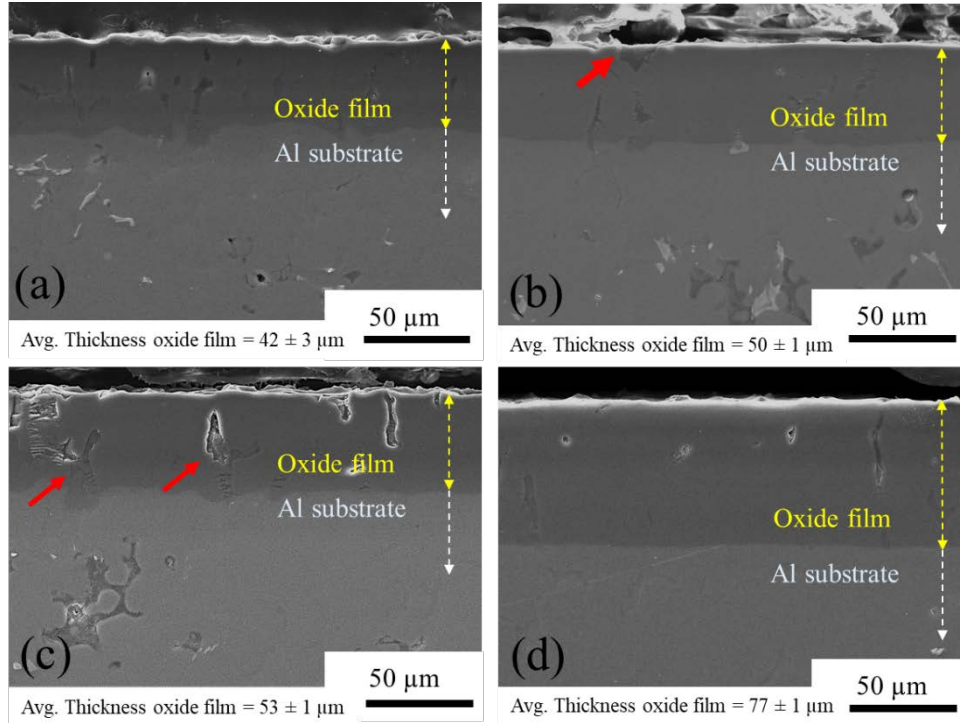


**Fig.5** Anodic oxide film thickness in different conditions: (a) as-cast-CA, (b) as-homogenized with anodizing-HA, (c) as-cast, anodized and sealed stearic-CAS, (d) as-homogenized, anodized and sealed stearic-HAS (Quantitative result of film thickness is in each figure). The red arrow indicates the intermetallic embedded in the anodic oxide film.

The surface morphology of the anodic oxide film in the as-cast and homogenized alloys after anodizing and sealing with stearic acid is given in Fig. 6. One can see that the as-cast alloy seems to have cracks or grooves of intermetallics, which can be explained by the interrupted growth of oxide film during anodizing treatment (Fig. 6a). While these cracks can be sealed by stearic film, white texture of uneven stearic sealing film could be still seen on the oxide surface in Fig. 6 (c). Interestingly the surface morphology of the anodic oxide film in the HAS specimen exhibited obvious petal-shaped sealing pattern on the anodic oxide film as can be seen in Fig. 5(d). This might result from less intermetallics on the surface after homogenization (Fig. 5(b)) that activated the growth rate of the oxide film [15, 16], which was further promoted by the chemical reaction of stearic sealing process, forming a sealing film layer. It was reported that the Al surface tends to be oxidized in a humid atmosphere, and in particular an acid environment will release  $\text{Al}^{3+}$  that can later react with  $\text{O}^{2-}$  to form the oxide  $\text{Al}_2\text{O}_3$  [17]. This may be the reason of the higher oxide film thickness in the homogenized alloy with stearic sealing.

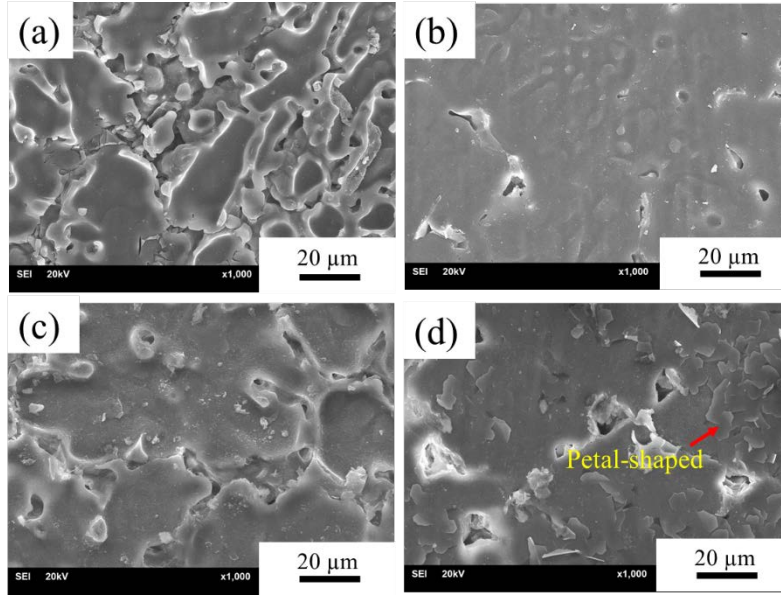


**Fig.6** Surface morphology of anodic oxide film with and without sealing of stearic sealant; (a) CA, (b) HA, (c) CAS and (d) HAS

The corrosion behavior of an A535 alloy was evaluated through the potentiodynamic polarization curve. In general, the polarization dynamic curve showed that the corrosion potentials in all experimental alloys was not significantly different in the active region, but the corrosion behavior became different in the passivation region, which can be discussed in terms of the oxide film and the stability of passive film in 5% wt NaCl as shown in Fig. 7(a).

The corrosion density ( $I_{\text{corr}}$ ) significantly decreased in the homogenized alloy with anodizing (HA sample) as compared to the as-cast alloy with anodizing (CA sample). This may be due to the presence of  $\text{Al}_3\text{Mg}_2$  and  $\text{Mg}_2\text{Si}$  intermetallics in the as-cast alloy that have a low corrosion potential of about (-1.3V)-(-1.5V) vs the saturated calomel electrode (SCE) that commonly acts as an active cathodic electrode [3, 18]. As the corrosion reaction goes, the oxide film degrades and the oxidation reaction of the active intermetallic  $\text{Al}_3\text{Mg}_2$  takes place with the electrolytic solution.

However, the detrimental effect of intermetallics can be alleviated by the sealing effect of stearic acid. It is clearly seen that the anodized as-cast alloy with stearic sealing (CAS) has higher corrosion potential ( $E_{\text{corr}} = -0.6 \text{ V}$ ) in the active region as compared to the homogenized alloy (HAS) that has  $E_{\text{corr}}$  value of  $-0.9 \text{ V}$ , which indicates that the metal oxidation is low at the initial stage of corrosion reaction. It was reported that the corrosion potential of the alloy depends on the type of an active intermetallic [18]. Although the as-cast alloy has a large number of intermetallics, the  $E_{\text{corr}}$  of this alloy decreased from  $-0.9 \text{ V}$  (CA) to  $-0.6 \text{ V}$  (CAS) as can be seen in Fig. 7 (c). This is because of the effect of stearic sealing that covers the surface at the beginning of reaction. The decrease in corrosion potential ( $E_{\text{corr}}$ ) is probably due to the reduction in the rate of anodic reaction as a result of the formation of a superhydrophobic stearic sealing film on the anodic oxide surface [19]. On the other hand, the homogenized alloy with stearic sealing (HAS) has slightly lower the value of  $E_{\text{corr}}$  ( $-0.92 \text{ V}$ ) than the CAS alloy ( $-0.6 \text{ V}$ ) in the beginning of the active region. This may be caused by corrosion and cracking of the petal-shaped stearic sealing film in the beginning stage, but the passive oxide film of the HAS alloy is the most stable corrosion reaction in passivation



region as can be seen in the HAS curve of Fig. 7(a). When the alloy was homogenized and sealed with stearic acid, it had the lowest corrosion current of about  $1\text{E-}10\text{ A/cm}^2$  as compared to others (Fig. 7(b)). That is a result of the corrosion resistance of the stearic sealed film being quite good as the stearic acid sealed film has a relatively low passive current [20]. However, it is interesting to note that even the homogenized alloy had a higher corrosion potential in the active stage as can be seen in Fig.7 (a), but showed a more stable passive film in the passivation region attested by the flat part of the HA curve, indicating that a passive film could form to prevent the corrosion reaction. This resulted in the lowest of corrosion rate in the homogenized and sealed alloy (Fig. 7(d)).

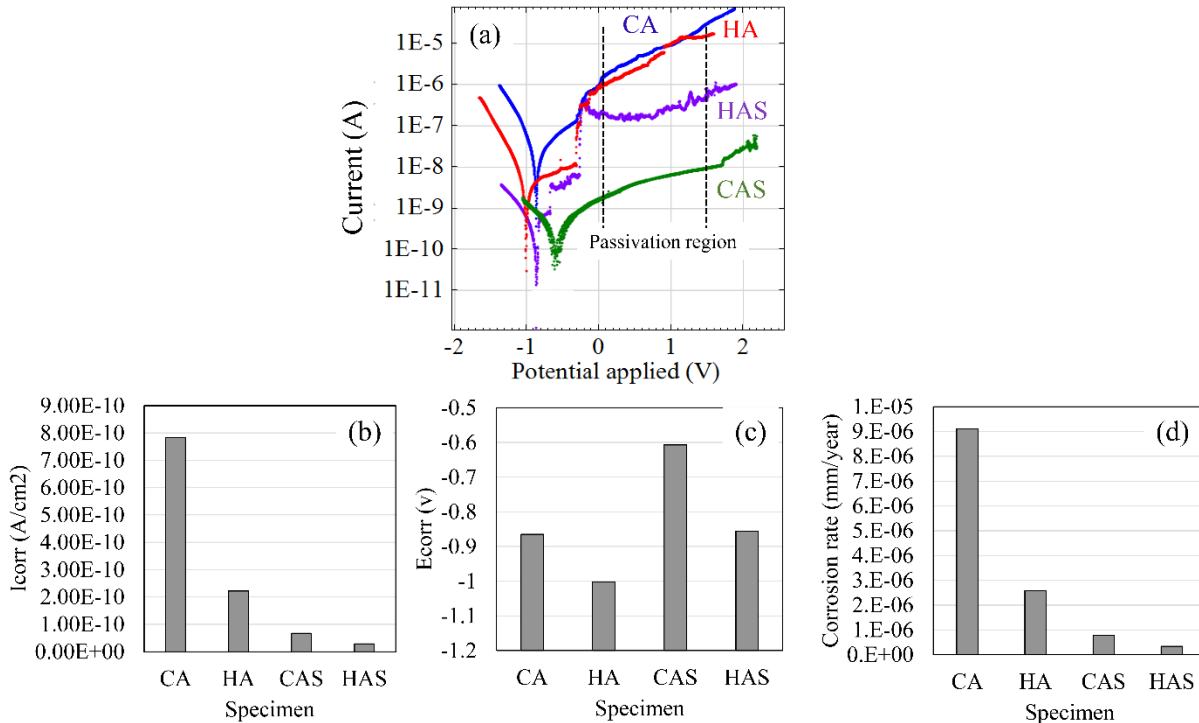


**Fig.7** Potentiodynamic polarization curves in 5% NaCl; (a) A typical potentiodynamic-polarization curve, (b) corrosion current density ( $I_{corr}$ ), (c) corrosion potential ( $E_{corr}$ ), and (d) the calculated results of corrosion rate

## Conclusions

The present study highlights the promising results obtained with an A535 aluminum-magnesium casting alloy with homogenization treatment at  $400\text{ }^\circ\text{C}$  for 5-7 hours. The dissolution of intermetallics provided the uniform anodic oxide film with stearic sealing, which was clearly revealed by the significant enhancement of hardness and corrosion resistance. As a result of this study, we came to the following conclusions.

1. The homogenization treatment at  $400\text{ }^\circ\text{C}$  for 5 hour is suitable to dissolve the intermetallics in an A535 aluminum–magnesium alloy.
2. The hardness of the alloy significantly increased after homogenization at  $400\text{ }^\circ\text{C}$  for 5 hour due to the solid solution strengthening of the Al matrix.
3. The uniformity of the anodic films is influenced by the presence of intermetallics in as-casting alloy.



4. The combined effect of homogenization and stearic acid sealing can improve the stability of anodic oxide film in 5wt% NaCl solution, which improves the corrosion resistance of the alloy.

## Acknowledgements

The authors are grateful for the Research Strengthening the Project of Faculty of Engineering, KMUTT year 2563 and Thailand Science Research and Innovation (TSRI) under Fundamental Fund 2022 for financial support. The authors also would like to thank the Department of Tool and Materials Engineering and Production Engineering Department, King Mongkut's University of Technology Thonburi laboratory facilities. FE-SEM center at school of engineering, King Mongkut's Institute of Technology Ladkrabang.

## References

- [1] F. Fasoyinu, J. Thomson, T. Castles, M. Sahoo (2003) Mechanical properties and metallography of Al-Mg alloy 535.0, AFS Transactions 3(115), 1-13.
- [2] F. Fasoyinu, D. Cousineau, M. Sahoo (2005) Marrying Almag 535 to the permanent mold process, Modern Casting 95(1), 43-45.
- [3] R. Jones, D. Baer, M. Danielson, J. Vetrano (2001) Role of Mg in the stress corrosion cracking of an Al-Mg alloy, Metall Mater Trans A 32(7), 1699-1711.
- [4] C. Berlanga-Labari, M.V. Biezma-Moraleda, P.J. Rivero (2020) Corrosion of cast aluminum alloys: a review, Metals 10(10), 1384.
- [5] G. Boisier, A. Lamure, N. Pèbère, N. Portail, M. Villatte (2009) Corrosion protection of AA2024 sealed anodic layers using the hydrophobic properties of carboxylic acids, Surface and Coatings Technology 203(22), 3420-3426.
- [6] J.M. Runge (2018) The Metallurgy of Anodizing Aluminum: Connecting Science to Practice, Springer.
- [7] J.M. Runge, T. Hossain (2015) Interfacial phenomena in 7000 series alloys and their impact on the anodic oxide, Materials Today: Proceedings 2(10), 5055-5062.
- [8] V.S. Zolotarevsky, N.A. Belov, M.V. Glazoff (2007) Casting Aluminum Alloys, Elsevier, Oxford
- [9] S. Samaras, G. Haidemenopoulos (2007) Modelling of microsegregation and homogenization of 6061 extrudable Al-alloy, Journal of Materials Processing Technology 194(1-3), 63-73.
- [10] ASM Handbook (1991). Vol. 4: Heat Treating, ASM Standards, American Society for Metals, Materials Park, OH.
- [11] G102-89 (2004) Calculation of Corrosion Rates and Related Information from Electrochemical Measurements, Annual Book of ASTM Standards, ASTM International, West Conshohocken, PA.
- [12] C. T. Wu, S. L. Lee, Y. F. Chen, H. Y. Bor, K. H. Liu (2020) Effects of Mn, Zn additions and cooling rate on mechanical and corrosion properties of Al-4.6 Mg casting alloys, Materials 13(8), 1983.
- [13] M.S. de Miera, M. Curioni, P. Skeldon, G. Thompson (2010) The behaviour of second phase particles during anodizing of aluminium alloys, Corrosion Science 52(7), 2489-2497.
- [14] Y. Shang, L. Wang, Z. Liu, D. Niu, Y. Wang, C. Liu (2016) The effects of different sealing techniques for anodic film of Al.-12.7 Si-0.7 Mg Alloys, Int J Electrochem Sci 11, 5234-5344.

- [15] H. Shi, M. Yu, J. Liu, G. Rong, R. Du, J. Wang, S. Li (2020) Effect of alkaline etching on microstructure and anticorrosion performance of anodic film on Al-Mg-Si alloy, *Corrosion Science* 169, 108642.
- [16] O. Engler, K. Kuhnke, J. Hasenclever (2017) Development of intermetallic particles during solidification and homogenization of two AA 5xxx series Al-Mg alloys with different Mg contents, *J Alloys and Compounds* 728, 669-681.
- [17] D. Zang, R. Zhu, W. Zhang, J. Wu, X. Yu, Y. Zhang (2014) Stearic acid modified aluminum surfaces with controlled wetting properties and corrosion resistance, *Corrosion Science* 83, 86-93.
- [18] K. Yasakau, M. Zheludkevich, M. Ferreira (2018) Role of intermetallics in corrosion of aluminum alloys. In: *Intermetallic Matrix Composites*, Woodhead Publ., 425-462.
- [19] M. Mirzadeh, K. Dehghani, M. Rezaei, Z. Mahidashti (2019) Effect of stearic acid as a low cost and green material on the self-cleaning and anti-corrosion behavior of anodized titanium, *Colloids and Surfaces A: Physicochemical and Engineering Aspects* 583, 123971.
- [20] Y. Zuo, P.-H. Zhao, J.-M. Zhao (2003) The influences of sealing methods on corrosion behavior of anodized aluminum alloys in NaCl solutions, *Surface and Coatings Technology* 166(2-3), 237-242.